Multiple-scattering and DV-Xα analyses of a Cl-passivated Ge(111) surface

2003 J. Phys.: Condens. Matter 15 5261

(http://iopscience.iop.org/0953-8984/15/30/308)

INSTITUTE OF PHYSICS PUBLISHING JOURNAL OF PHYSICS: CONDENSED MATTER

J. Phys.: Condens. Matter **15** (2003) 5261–5268 PII: S0953-8984(03)61039-8

Multiple-scattering and DV-Xα analyses of a Cl-passivated Ge(111) surface

S Cao[1,3], J-C Tang[1,2] and S-L Shen[1]

[1] Department of Physics, Zhejiang University, Hangzhou 310027, China
[2] State Key Laboratory for Silicon Material Science, Zhejiang University, Hangzhou 310027, China

E-mail: caosong@css.zju.edu.cn

Received 11 March 2003
Published 18 July 2003
Online at stacks.iop.org/JPhysCM/15/5261

Abstract

The multiple-scattering cluster and DV-Xα methods have been employed to analyse the chlorine 1s near edge x-ray absorption fine structure (NEXAFS) of a Cl-passivated Ge(111) surface. Our detailed analysis demonstrates how the chlorine atoms form a perfect monochloride structure with Cl bonding to the topmost Ge atom. Our calculation reveals the interaction in the chlorine layer is multipolar electrostatic forces. Furthermore, the DV-Xα cluster calculation shows that the orbital contour of the sharp Cl–Ge resonance exhibits a global symmetry, which confirms it to be σ^*-like. The above studies are found to enrich previous experimental NEXAFS investigations.

1. Introduction

In the world of semiconductors, silicon is, to a large part, king because silicon can be easily passivated by a simple thermal oxidation procedure. Other semiconductor materials such as Ge, InP and GaAs are technologically possible for many applications involved in microelectronic circuits, device fabrication and epitaxial growth [1–3]. The difficulty for their application is to obtain a stable and oxide-free semiconductor surface. Fortunately, well-ordered and air-stable GaAs(111) and Ge(111) surfaces have been obtained by passivation with HCl solution [4, 5]. The fact that Ge has a narrower bandgap than Si and high hole mobility makes it a potential candidate for high performance device manufacture [6]. Therefore the Cl-passivated Ge surface is very useful in industrial and technological applications.

In the past, NEXAFS (near edge x-ray absorption fine structure), EXAFS (extended x-ray absorption fine structure), first-principles and MSC (multiple-scattering cluster) calculations [7–9] have been successfully utilized to determine the structural information of Cl-passivated Ge surfaces. These studies unambiguously show a stable atop Cl–Ge

[3] Author to whom any correspondence should be addressed.

monochloride structure. The EXAFS analysis gives an average Cl–Ge bond length of 2.17±0.01 Å [7], the slab model and MSC calculation yield the results of 2.13 and 2.15±0.05 Å respectively [8, 9]. However, our previous work [9] focused on the atomic structure of a Cl-passivated Ge(111) surface, while the electronic structure of the chlorine layer and the Ge substrate were discussed very little. In this paper, we will investigate the interaction between the adsorbates and the substrates as well as the adsorbates themselves by means of MSC calculations. Furthermore we will make a series of DV-Xα studies showing the electronic states information of the chlorine layer, which reveals some characteristics of the adsorbed chlorine layer.

2. The MSC and DV-Xα methods

In the NEXAFS process, a core level electron of an atom is excited by incident x-rays. The excited photoelectron is scattered by atoms surrounding the centre and then transits into the unoccupied antibonding states or the shape resonance states, or directly goes out of the system if the x-ray energy is high enough (photoemission). As is described above, the physical origin of NEXAFS and photoemission is similar. This allows us to utilize the dynamic theory of photoelectron diffraction to calculate the wavefunction of an intermediate photoelectron in NEXAFS [10, 11], thereby computing the absorption cross section by the MSC method. A detailed derivation of the formalism can be found elsewhere [12, 13]. Inputs to the calculation of NEXAFS spectra include the position of atoms in the chosen cluster, the incident x-ray polarization and the atomic scattering phase shifts (corresponding to s, p, d waves), which are calculated by the self-consistent field (SCF) Xα method. For the calculation of the phase shifts a cluster muffin-tin (MT) potential with overlapping MT spheres has been used. The MT radii for the atoms are determined by the Norman criterion with about 10% overlapping factor [14], which can be directly obtained in the SCF Xα program.

To reveal the properties of the lower unoccupied molecular orbitals (LUMO + 1) of the cluster associated with the resonances in NEXAFS and compare them with the above MSC calculation, we perform a self-consistent DV-Xα calculation for the same system. The DV-Xα cluster method [15, 16] is one of the most useful techniques for solving the Harttree–Fock–Slater (HFS) equation based on a statistical approximation to the exchange–correlation potential. Recently, our group has successfully applied a DV-Xα calculation to connect the LUMO + 1 of a (SO + 2O) + 6Cu cluster with the individual resonances in NEXAFS spectra of a SO_2/Cu(100) system at 280 K [17]. By means of the DV-Xα method, we can calculate the cluster wavefunction and the corresponding molecular orbitals, which are useful in analysing the transition probability and identifying the resonance position in NEXAFS spectra.

3. Results and discussion

3.1. Stacking a perfect chloride layer on Ge(111)

Lu *et al* [7] suggested that the atop monochloride structure is formed on a Ge(111) surface by means of Cl K-edge NEXAFS, EXAFS analysis and first-principles calculations. The nearest Cl–Cl distance is elongated to 4.0 Å for matching the Ge(111) lattice parameter. In order to get a better understanding of the experimental NEXAFS data, especially to show each individual resonance in NEXAFS which is closely correlated with the chlorine atoms, we have performed a MSC calculation for a series of 2Cl models and plotted the calculated Cl 1s NEXAFS curves in figure 1, in which the bond lengths $L_{\mathrm{Cl-Cl}}$ vary between 3.0 and 5.0 Å. For making a direct comparison, the experimental NEXAFS spectra of [7] are plotted in the same figure. By a

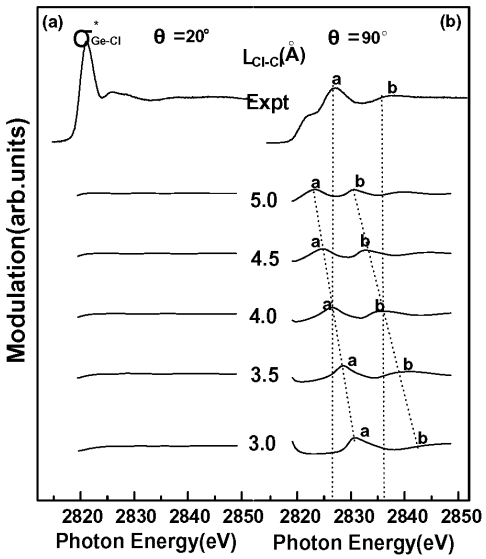

Figure 1. Comparison between the calculated chlorine K-edge NEXAFS spectra for different Cl–Cl bond lengths and the polarization dependent experimental spectra of a Cl-passivated Ge(111) surface [7]. The Cl–Cl bond lengths vary between 3.0 and 5.0 Å. The x-ray incidence angles are (a) $\theta = 15°$ and (b) $\theta = 55°$.

visual inspection, we can find the variation trend of the calculated NEXAFS spectra as follows. With the x-ray at grazing incidence, there are no features at all. However, two prominent wide resonances labelled 'a' and 'b' appear in the calculated curves as x-rays at normal incidence. These features shift to the lower energy with $L_{\mathrm{Cl-Cl}}$ elongated. It is shown that they are the shape resonances [18]. It should be point out that resonances a and b, of the calculated curve at incident angle $\theta = 90°$, correspond to the experimental spectrum one by one when the Cl–Cl distance arrives at 4.0 Å. Therefore, they are intrinsic features of the monochloride layer, which show that the Cl–Cl distance must be elongated to match the Ge(111) lattice constant in order to build a stable Cl/Ge(111) adsorption structure. This is the key point for the stability of Cl-passivated on a Ge(111) surface.

In order to exhibit the LUMO + 1 of the Cl–Cl distance elongated to 4.0 Å and to confirm the above MSC results, we perform a DV-Xα cluster calculation for the 2Cl model. The LUMO + 1 energy levels of the model contains little of the Cl(3p) component. We list three typical levels in table 1. These LUMO + 1 orbits consist of more than 98% 3d components. For example, the contour maps of energy level 15.37 eV are plotted in figure 2 on two planes, i.e. both the left and right ones are through the Cl–Cl axis but parallel to the [001] and [010] axes. By a visual inspection of figure 2, we find two Cl 3d orbitals located at isolated regions, so there is no hybridization between them. According to the electric dipole selection rule the intermediate photoelectron from the 1s core state cannot reach these orbitals, which means they do not correspond to the peaks a and b. In fact, the peaks a and b are the result of photoelectrons scattered between chlorine atoms. Usually the scattering features a and b are called shape resonances and are distinguished from the σ resonances which correspond to the LUMO levels in the DV-Xα calculation [13]. It is impossible to make a chemical bond between two Cl atoms which are so far apart. Therefore, the interaction between them is only multipolar electrostatic forces, for example, the dipole–dipole interaction which belongs to the van der Waals interaction.

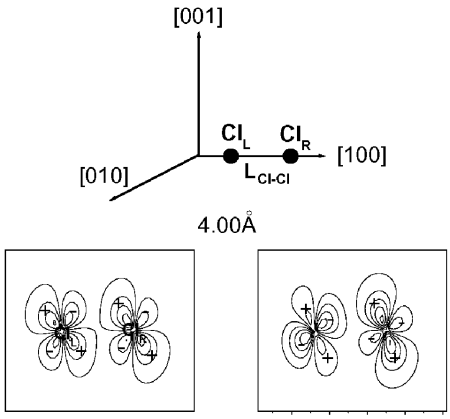

Figure 2. Contour maps of the molecular orbital of 15.37 eV with $L_{\mathrm{Cl-Cl}} = 4.0$ Å.

Table 1. Energy levels (eV) and orbital configuration of LUMO + 1 of $L_{\mathrm{Cl-Cl}} = 4.0$ Å.

Energy (eV)	The major configuration of the orbital	Assigned peaks
0.0	$Cl_L(3p)0.50$, $Cl_R(3p)0.50$	HOMO
14.25	$Cl_L(3d)0.83$, $Cl_R(3d)0.17$	Not
15.37	$Cl_L(3d)0.53$, $Cl_R(3d)0.47$	excited
15.90	$Cl_L(3d)0.24$, $Cl_R(3d)0.76$	

To further analyse the chlorine layer, we construct four cluster models to simulate the Cl-passivated process. These models consist of 2Cl, 4Cl, 7Cl and 13Cl (see figure 3). The calculated Cl 1s NEXAFS spectra of the above four models are shown in figure 4. By comparison of the curves for the former three cluster models, we find the intensities of peaks a and b depending on the number of Cl atoms. The greater number of Cl atom, the more intense peaks a and b will be. In order to fit the experimental ones, the number of chlorine atoms must increase until they contain a whole nearest-neighbour circle around the Cl centre. In addition, adding the second-neighbour circle has no effect on the calculated NEXAFS spectrum; it is unambiguously shown that chlorine atoms have formed a perfect monochloride layer on the Ge(111) surface where one Cl atom is surrounded by 6Cl neighbours with a Cl–Cl distance of 4.0 Å.

3.2. The chemical bond between chlorine and germanium

As mentioned above, there exists a sharp resonance in the experimental Cl 1s NEXAFS spectra when the x-ray is at grazing incidence [7], which is assigned as the $\sigma^*_{\mathrm{Ge-Cl}}$ peak. However it lacks direct theoretical identification. In what follows, we will perform MSC and DV-Xα cluster calculations to clarify this fact. We have calculated the Cl 1s NEXAFS spectra of two cluster models, i.e. $Cl_0 + Ge_0$ and $Cl_0 + 6Cl_1 + Ge_0$ (see figure 3(B)). The Cl_0 and Ge_0 bond length is 2.15 Å while the Cl atoms take the top sites. The comparison between the calculated curves and the experimental ones is shown in figure 5. It is clearly seen that the sharp peak appears in the $Cl_0 + Ge_0$ cluster at the grazing incidence, which is mainly derived from the Cl_0 bonding with the topmost Ge_0 atom. Moreover the DV-Xα cluster calculation is employed to approach the LUMO + 1 information of the $Cl_0 + Ge_0$ cluster. In the calculation, three

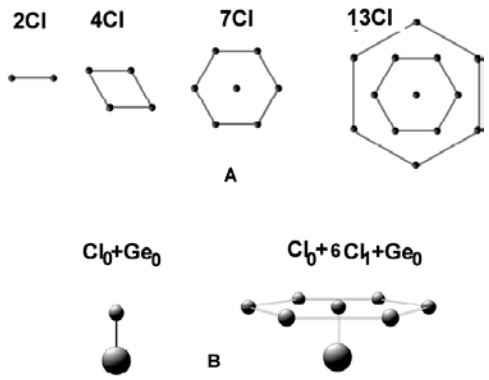

Figure 3. Schematic diagram for (A) four kinds of atom clusters corresponding to the calculated spectra plotted in figure 4, (B) two kinds of atom clusters corresponding to the calculated spectra plotted in figure 5.

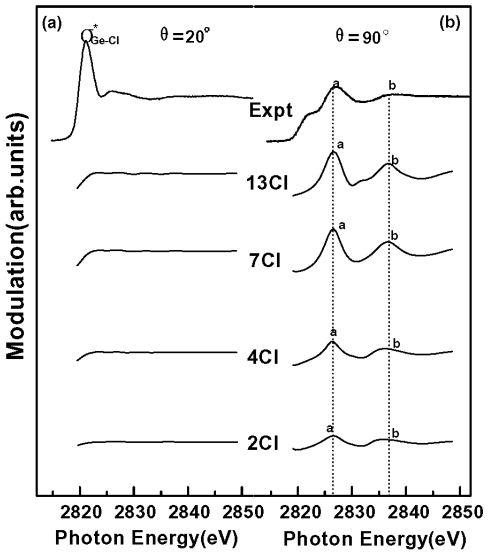

Figure 4. Comparison between the experimental spectra and calculated Cl K-edge NEXAFS spectra for four clusters which include 2, 4, 7 and 13 Cl atoms respectively. The x-ray incidence angles are (a) $\theta = 15°$ and (b) $\theta = 55°$.

hydrogen atoms are used to saturate the Ge_0 dangling bonds. The H–Ge bond length is set to 1.55 Å. The scheme is done for following the DV-Xα cluster calculation. Other structural parameters are similar to those for the MSC calculation. The typical LUMO + 1 energy levels of the $Cl_0 + Ge_0$ cluster are listed in table 2(A). The lowest unoccupied molecular orbital corresponds to the σ^*_{Ge-Cl} resonance. We plot its contour maps in the upper panel of figure 6 in which 1-σ-1 and 1-σ-2 represent two planes being parallel to the [100] and [010] axes, while both are through the Cl_0-Ge_0 axis. The orbital displays approximate global symmetry around the Cl_0-Ge_0 bond, which suggests that the Cl and Ge peak is σ^*-like.

Furthermore, when we add six other surrounding Cl_1 atoms to the above cluster (i.e. $Cl_0 + 6Cl_1 + Ge_0$) the σ^*_{Ge-Cl} peak is little effected in spite of the peaks a and b appearing.

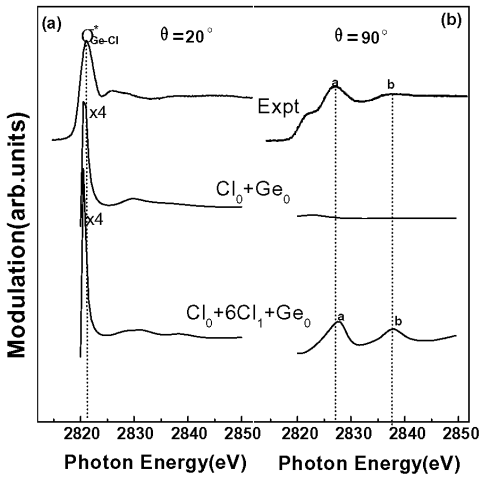

Figure 5. Comparison between the experimental spectra and calculated Cl K-edge NEXAFS spectra for two clusters: $Cl_0 + Ge_0$ and $Cl_0 + 6Cl_1 + Ge_0$ respectively. The x-ray incidence angles are (a) $\theta = 15°$ and (b) $\theta = 55°$.

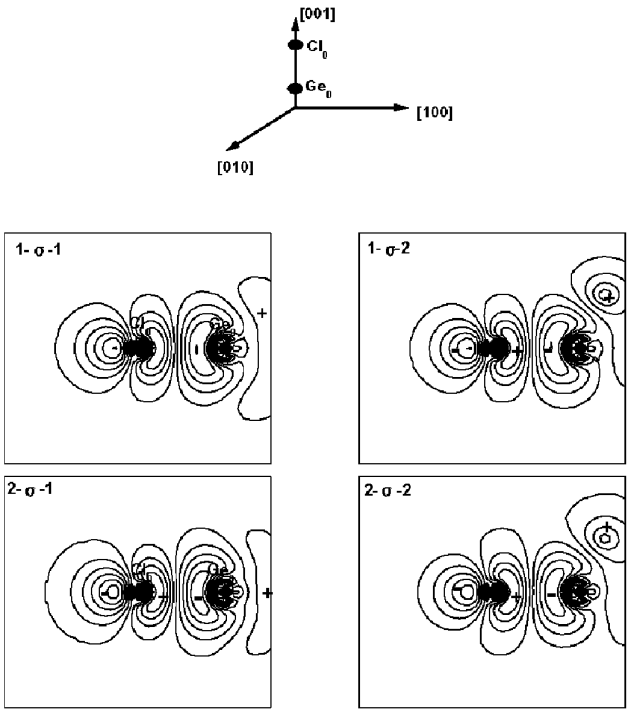

Figure 6. Contour maps of the lowest unoccupied orbital of $Cl_0 + Ge_0$ and $Cl_0 + 6Cl_1 + Ge_0$ associated with the peak in figure 5.

Its typical LUMO + 1 levels are listed in table 2(B). The energy level located at 6.74 eV corresponds to σ^*_{Ge-Cl}, whose contour maps exhibit an approximate global symmetry around

Table 2. Energy levels (eV) and orbital configuration of LUMO + 1 of $Cl_0 + Ge_0$ and $Cl_0 + 6Cl_1 + Ge_0$ clusters.

Energy (eV)	The major configuration of the orbital	Assigned peaks
	A. $Cl_0 + Ge_0$	
0.0	$Cl_0(3p)0.91$, $Ge_0(3s)0.09$	HOMO
6.95	$Cl_0(3p)0.27$, $Cl_0(3d)0.09$, $Ge_0(4s)0.21$, $Ge_0(4p)0.23$, $H(1s)0.17$	σ^*_{Cl-Ge}
9.60	$Cl_0(3p)0.03$, $Ge_0(4s)0.11$, $Ge_0(4p)0.41$, $H(1s)0.44$	Weakly
9.84	$Cl_0(3p)0.02$, $Cl_0(3d)0.21$, $Ge_0(4p)0.44$, $H(1s)0.32$	excited
10.08	$Cl_0(3p)0.02$, $Cl_0(3d)0.22$, $Ge_0(4p)0.44$, $H(1s)0.32$	
14.40	$Cl_0(3d)0.99$	Not
15.85	$Cl_0(3d)0.76$, $Ge_0(4p)0.18$, $H(1s)0.06$	excited
16.58	$Cl_0(3d)0.90$, $Ge_0(4s)0.03$, $Ge_0(4s)0.06$	
	B. $Cl_0 + 6Cl_1 + Ge_0$	
0.0	$Cl_1(3p)0.99$	HOMO
6.74	$Cl_0(3p)0.27$, $Cl_0(3d)0.09$, $Ge_0(4s)0.19$, $Ge_0(4p)0.27$, $H(1s)0.16$	σ^*_{Cl-Ge}
9.68	$Cl_0(3p)0.02$, $Cl_0(3d)0.03$, $Ge_0(4s)0.11$, $Ge_0(4p)0.39$, $H(1s)0.45$	Weakly
9.92	$Cl_0(3p)0.02$, $Cl_0(3d)0.20$, $Ge_0(4p)0.42$, $H(1s)0.34$	excited
10.06	$Cl_0(3p)0.02$, $Cl_0(3d)0.24$, $Ge_0(4p)0.42$, $H(1s)0.31$	
13.57	$Cl_0(3d)0.40$, $Cl_1(3d)0.60$	Not
14.76	$Cl_0(3d)0.02$, $Cl_1(3d)0.97$	excited
15.83	$Cl_0(3d)0.16$, $Cl_1(3d)0.83$	
15.98	$Cl_0(3d)0.54$, $Ge_0(4p)0.11$, $Cl_1(3d)0.31$	
16.90	$Cl_0(3d)0.76$, $Ge_0(4s)0.02$, $Ge_0(4p)0.05$, $Cl_1(3d)0.15$	

the Cl_0-Ge_0 bond as shown in figure 6 (2-σ-1, 2-σ-2). The definition of the two planes is similar to those of the former. Comparing these two calculation results, we find that the sharp resonance is attributed to the $Cl_0 + Ge_0$ cluster, which is excited at grazing incidence, while the scattering resonances a and b are due to the Cl layer and excited at normal incidence.

4. Conclusions

We have investigated the Cl K-shell NEXAFS spectra of Cl-passivated on a Ge(111) surface by both the MSC and DV-Xα methods. Our detailed analysis shows how the chlorine atoms form a perfect Cl monolayer on the Ge(111) surface where one Cl atom is surrounded by 6Cl neighbours with a Cl–Cl distance of 4.0 Å. The interaction between the centre Cl_0 and the neighbour Cl_1 is multipolar electrostatic forces, for example, the dipole–dipole interaction. The photoelectrons scattered in the chlorine layer form the intrinsic peaks a and b, which are shape resonances. Every chloride atom in the chloride layer bonds to the topmost Ge_0 atom, which contributes to the first sharp σ^*_{Ge-Cl} resonance. The strong Cl–Ge bonding maintains the Cl-passivated Ge(111) adsorption surface stable.

Acknowledgment

The authors acknowledge the support of the National Natural Science Foundation of China, Grant No 10274068.

References

[1] Travis J 1993 *Science* **262** 1819
[2] Driad R, Lu Z H, Charbonneau S, McKinnon W R, Laframboise S, Poole P J and McAlister S P 1998 *Appl. Phys. Lett.* **73** 665
[3] Anderson G W, Hanf M C and Norton P R 1995 *Phys. Rev. Lett.* **74** 2764
[4] Lu Z H, Chatenoud F, Dion M M, Graham M J, Ruda H E, Koutzarov I, Liu Q, Mitchell C E J, Hill I G and McLean A B 1996 *Appl. Phys. Lett.* **67** 670
[5] Lu Z H 1996 *Appl. Phys. Lett.* **68** 520
[6] Sze S M 1981 *Physics of Semiconductor Devices* (New York: Wiley)
[7] Lu Z H, Tyliszczak T, Hitchcock A P and Dharma-wardana M W C 1999 *Surf. Sci.* **442** L948
[8] Dharma-wardana M W C, Zgierski M Z, Ritchie D, Jiang G P and Ruda H 1999 *Phys. Rev.* B **59** 15766
[9] Cao S, Tang J-C, Wang L, Zhu P and Shen S L 2002 *Surf. Sci.* **505** 286
[10] Tang J C, Fu S B, Ji H and Chen Y B 1992 *Sci. China* A **35** 965
[11] Fujikawa T 1981 *J. Phys. Soc. Japan* **50** 1321
[12] Tang J C, Feng X S, Shen J F, Fujikawa T and Okazawa T 1991 *Phys. Rev.* B **44** 13018
[13] Cao S, Tang J-C, Zhu P, Wang L and Shen S L 2002 *Phys. Rev.* B **66** 045403
[14] Norman J G Jr 1976 *Mol. Phys.* **31** 1191
[15] Averill F W and Ellis D E 1973 *J. Chem. Phys.* **59** 6412
[16] Adachi H, Tsukada M and Satoko C 1978 *J. Phys. Soc. Japan* **45** 875
[17] Zhu P, Tang J C and He J P 2000 *J. Phys. Chem.* B **104** 10597
[18] Stöhr J 1992 *NEXAFS Spectroscopy (Springer Series in Surface Science vol 25)* ed R Gomer (Berlin: Springer)